

Quantum Cascade Detector at 5 micrometers

C. Koeniguer, A. Gomez, A. Nedelcu, M. Carras, X. Marcadet and V. Berger

Matériaux et Phénomènes Quantiques
University Paris Diderot Paris 7

Thales Research and Technology



Presentation of the device

- Principle of a QCD
- Description of the sample

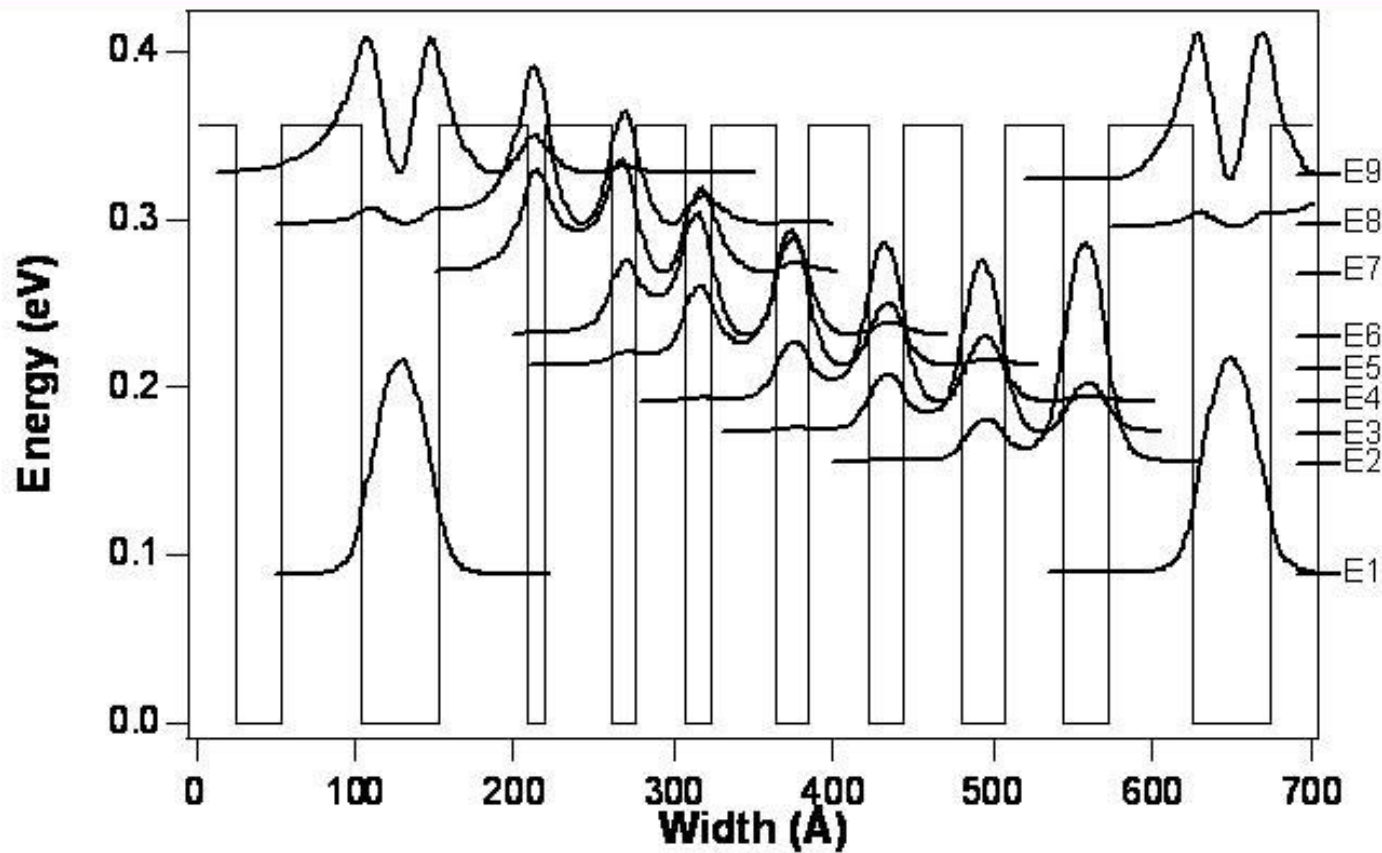
Characterization of the QCD

- Absorption and responsivity spectra
- Resistivity
- Noise and detectivity

Modeling of electronic transport

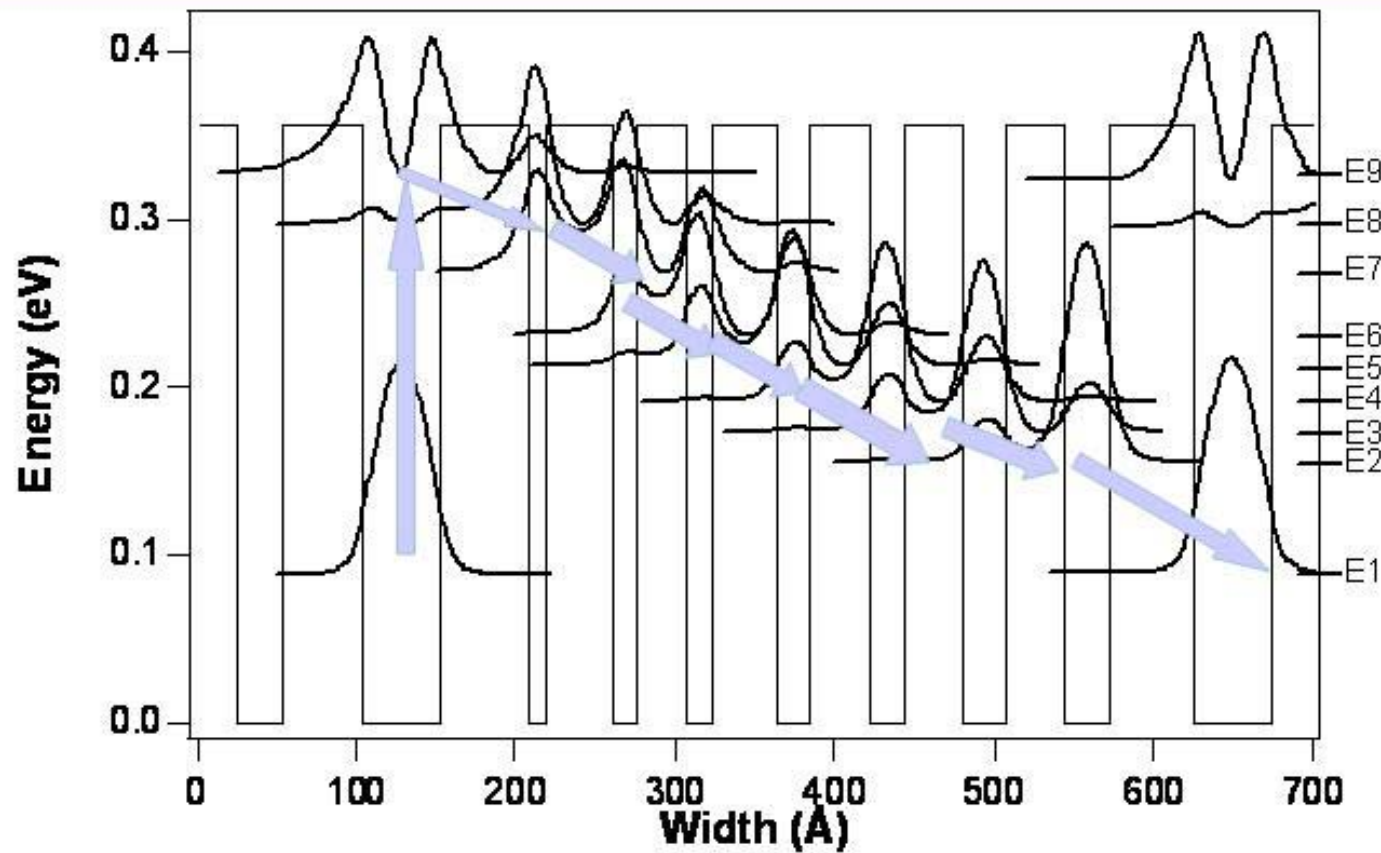
- Presentation of the model
- Some results and discussion
- QCD vs QWIP





- 40 periods of 8 barriers and quantum wells
- Quantum Wells : GaAs, thickness between 11 and 30 Å
- Barriers : AlGaAs, 44% Al, thickness between 30 and 60 Å
- 1st Quantum Well Si n-doped : $N_d = 5 \cdot 10^{11} \text{ cm}^{-2}$





- Thales patent “Détecteurs à cascade quantiques” (2001)
- Many QCDs have been demonstrated at Neuchatel (2.5 μm , 5.3 μm , 9 μm , 16.5 μm , 84 μm) and Paris (8 μm and 5.7 μm)

This document and any other data included herein are the property of Thales. They cannot be reproduced, distributed, used without Thales' prior written approval. © THALES 2006. Révisé: Modern version: 10.2





Presentation of the device

- Principle of a QCD
- Description of the sample

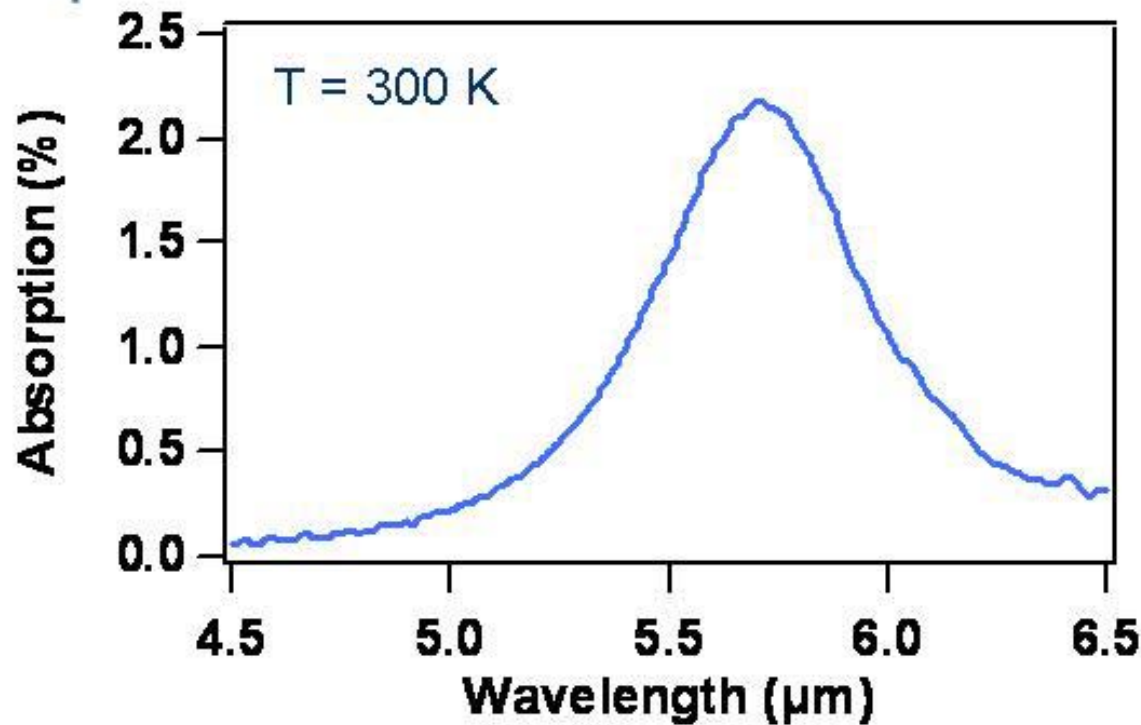
Characterization of the QCD

- Absorption and responsivity spectra
- Resistivity
- Noise and detectivity

Modeling of electronic transport

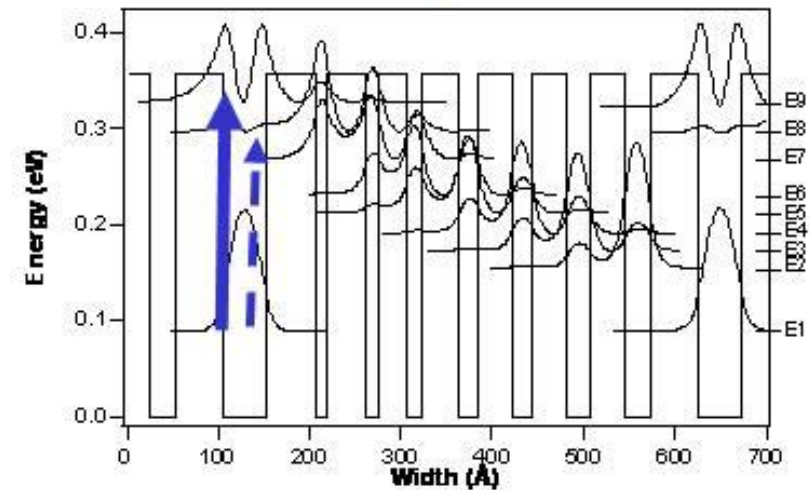
- Presentation of the model
- Some results and discussion





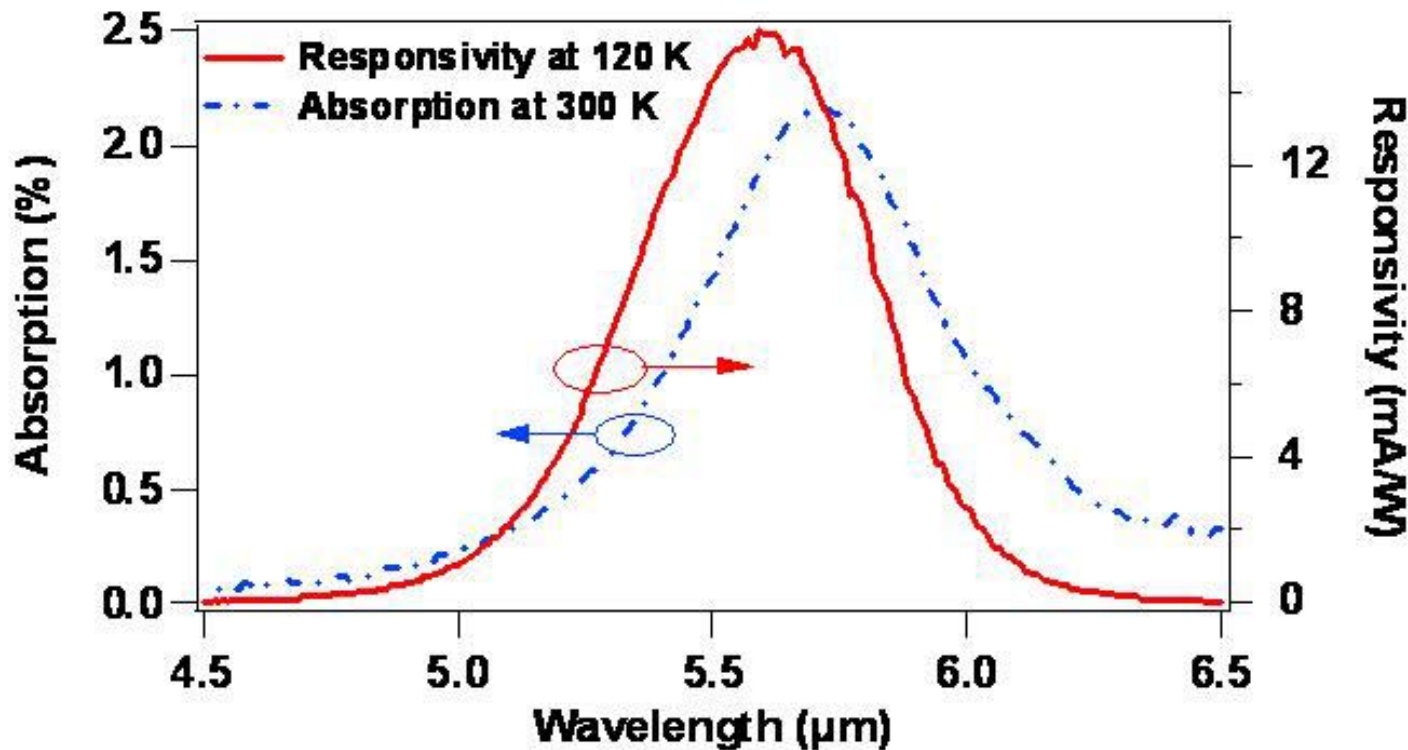
Absorption peak :

$$\lambda = 5.7 \mu\text{m}$$



- Multipath absorption measurement on a full wafer
- Doping concentration deduced from absorption coefficient :
 $N_d = 10^{12} \text{ cm}^{-2}$
- % Al deduced from DDX measurement : 47 %

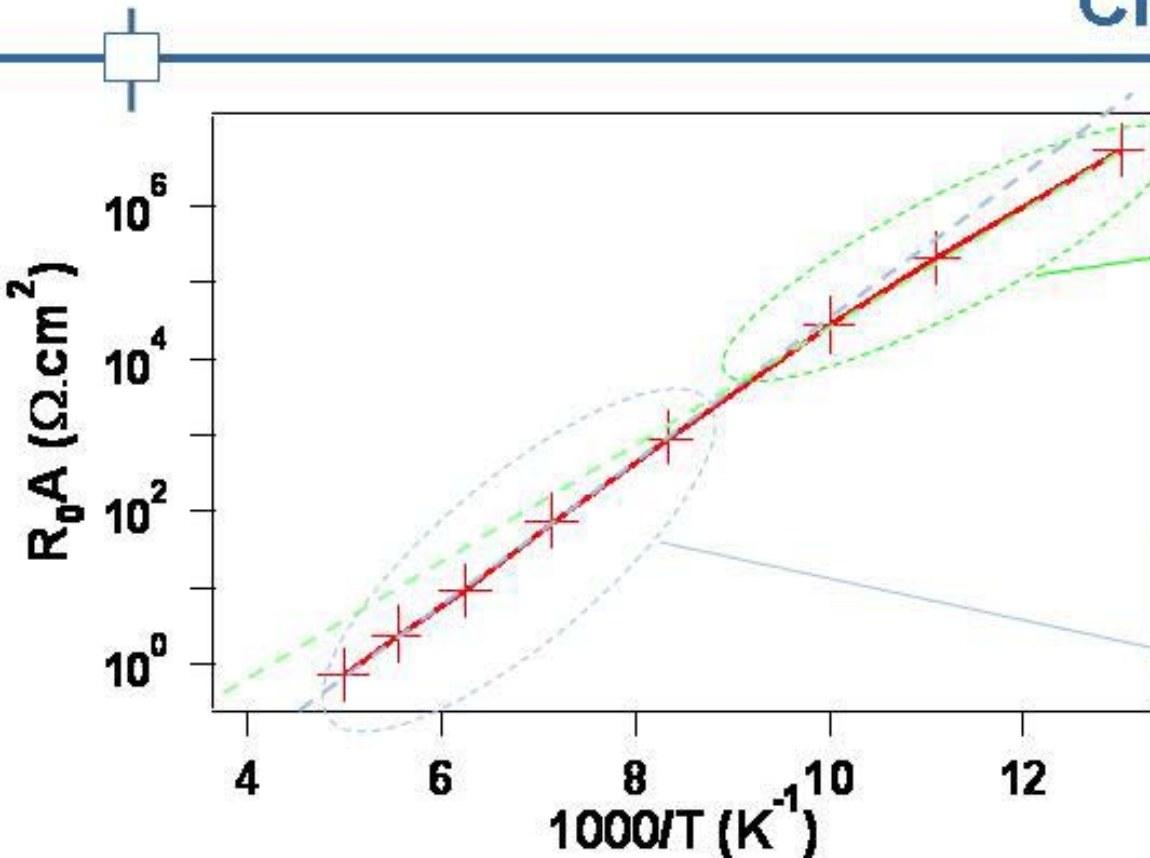




Responsivity at peak, for a $100\mu\text{m}\times 100\mu\text{m}$ pixel, at 120 K, at 0 V and with an optical coupling grating :

$$R = 15 \text{ mA/W}$$





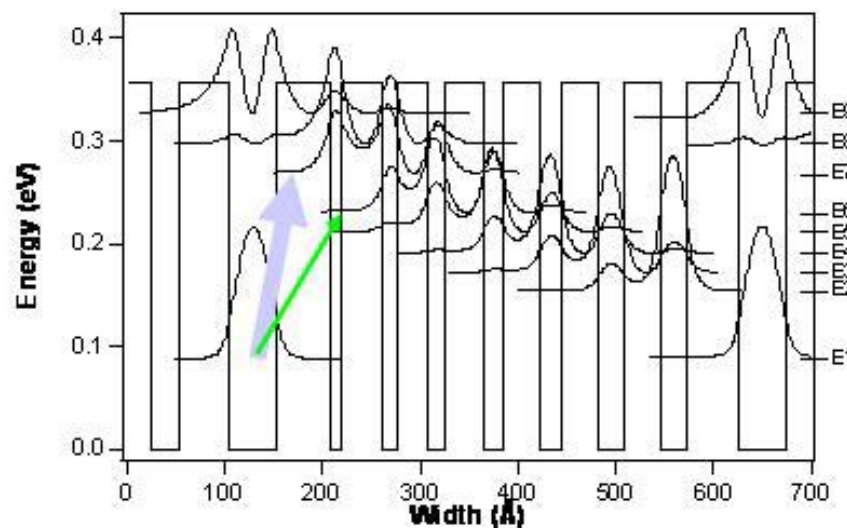
Activation energy $E_a \approx 150$ meV

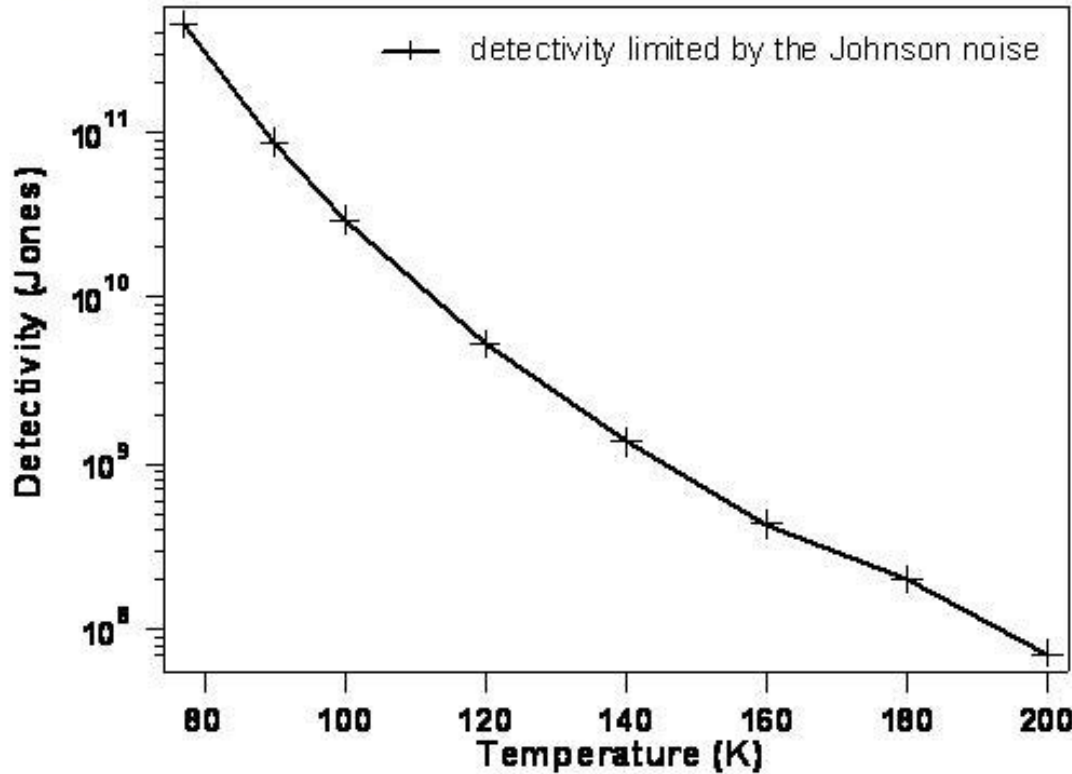
Transition E1 - E6

Activation energy $E_a \approx 180$ meV

Transition E1 - E7

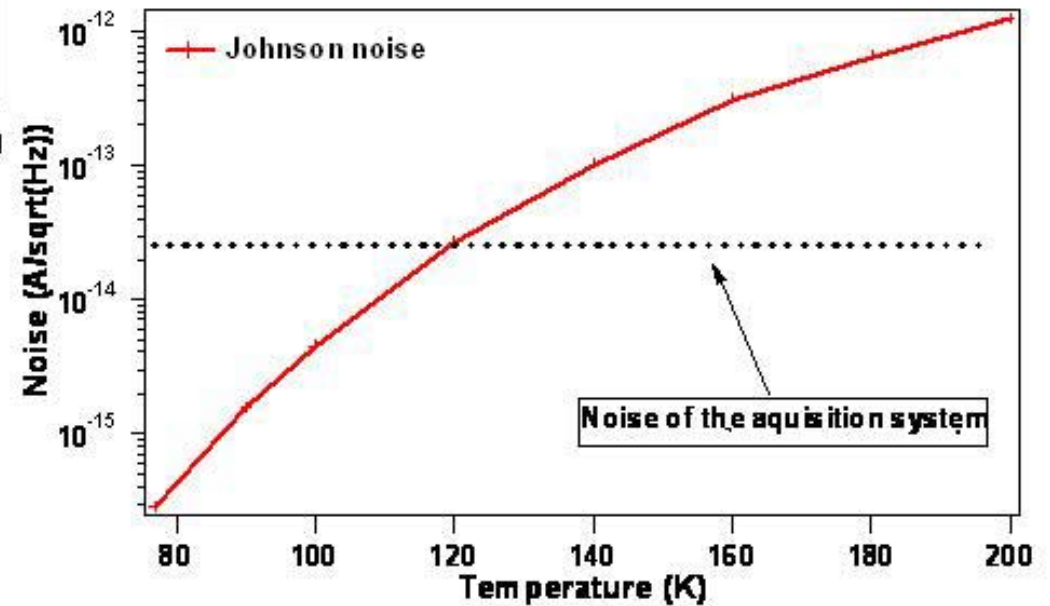
- High resistivity :
 - $5 \cdot 10^6 \Omega \cdot \text{cm}^2$ @ 77 K
 - $2.7 \cdot 10^4 \Omega \cdot \text{cm}^2$ @ 100 K
- leakage current due to transition toward a high energy level (E7)





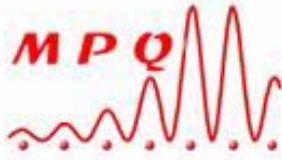
$D^* = 1.2 \cdot 10^9$ Jones
 at 140 K, for a 100 μ m square mesa, with an optical coupling grating, at 0V

- One order of magnitude lower than MCT
- Due to lower quantum efficiency (same situation than QWIPS)



This document and any other information included herein are the property of Thales. They cannot be reproduced, distributed or used without Thales' authorization. © THALES 2006. Révisé: Niveau: version: 10.2

ITQW 2007





Presentation of the device

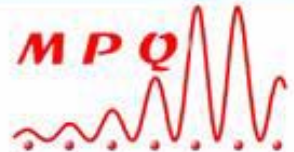
- Principle of a QCD
- Description of the sample

Characterization of the QCD

- Absorption and responsivity spectra
- Resistivity
- Noise and detectivity

Modeling of electronic transport

- Presentation of the model
- Some results and discussion



- 1 \Rightarrow Electron/LO-phonons interaction = dominant scattering process

- 2 \Rightarrow The electronic mobility is higher inside a cascade than between two consecutive cascades
 - \blacktriangledown Intra and inter-cascade transitions classification
 - \blacktriangledown Introduction of quasi Fermi levels associated with each cascade

- 3 \Rightarrow Low applied bias (calculation of R_0A , and photovoltaic operation) : The electric field will be considered as a perturbation





1 \Rightarrow Predominant scattering process : Electron/LO-phonons interaction

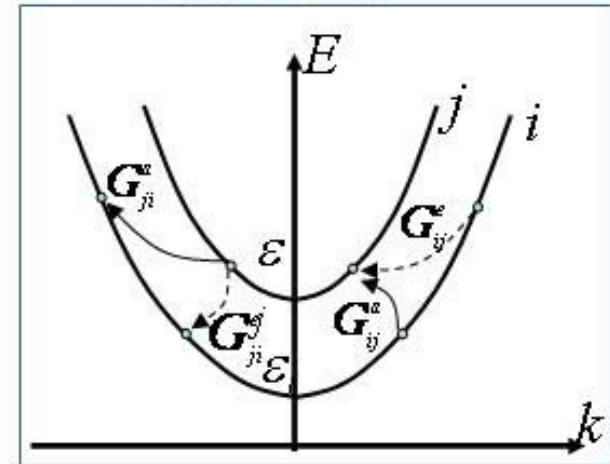
- Neglected scattering mechanisms :
- Interface roughness scattering
 - Acoustic phonons scattering
 - Electron-electron interactions

May not be true at very low temperature (see Leuliet et al. Phys. Rev. B 2006)

- not a problem for infrared detection application

$$G_{ij}^a = \int_{\epsilon_j - \hbar\omega_{LO}}^{\infty} S_{ij}^a(E) f(E) (1 - f(E + \hbar\omega_{LO})) n_{opt} D(E) dE$$

$$G_{ij}^e = \int_{\epsilon_j + \hbar\omega_{LO}}^{\infty} S_{ij}^e(E) f(E) (1 - f(E - \hbar\omega_{LO})) (1 + n_{opt}) D(E) dE$$

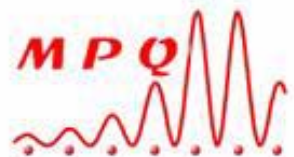


- S_{ij}^* single state transition rate to subband j
- G_{ij} global transition rate from subband i to subband j

At thermodynamical equilibrium :

$$G_{ij}^a = G_{ji}^e$$

\Rightarrow The net current is zero

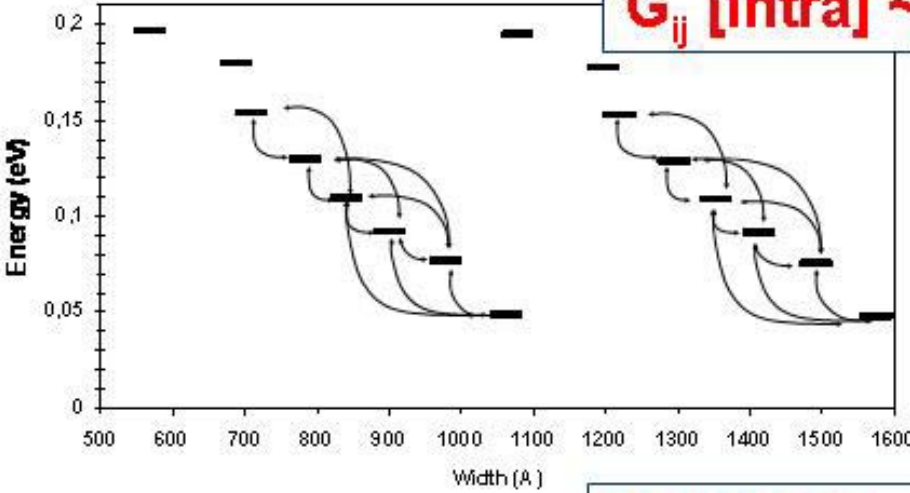




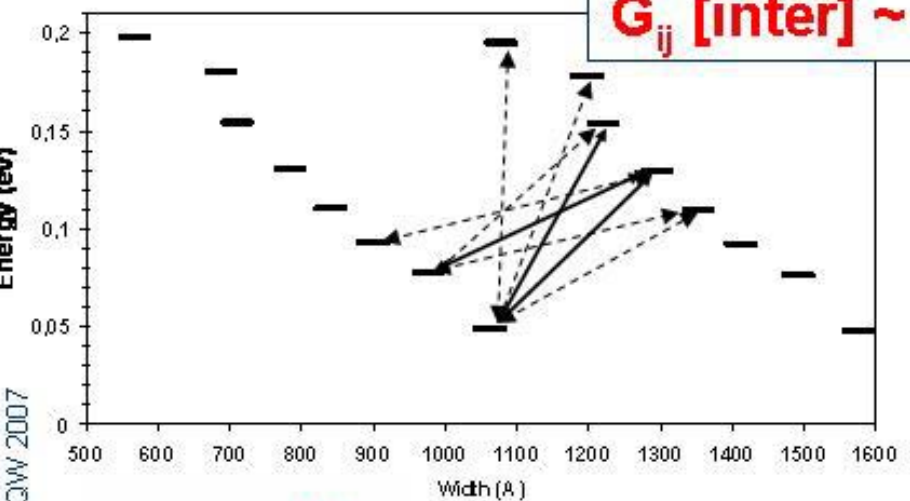
2 \Rightarrow Under bias, each cascade keeps its own quasi Fermi level

$$G_{ij} [\text{intra}] \sim 10^{20} / 10^{25} \text{ m}^{-2}\text{s}^{-1}$$

- $G_{ij} [\text{intra}] > G_{ij} [\text{inter}]$
- each cascade at quasi thermodynamical equilibrium

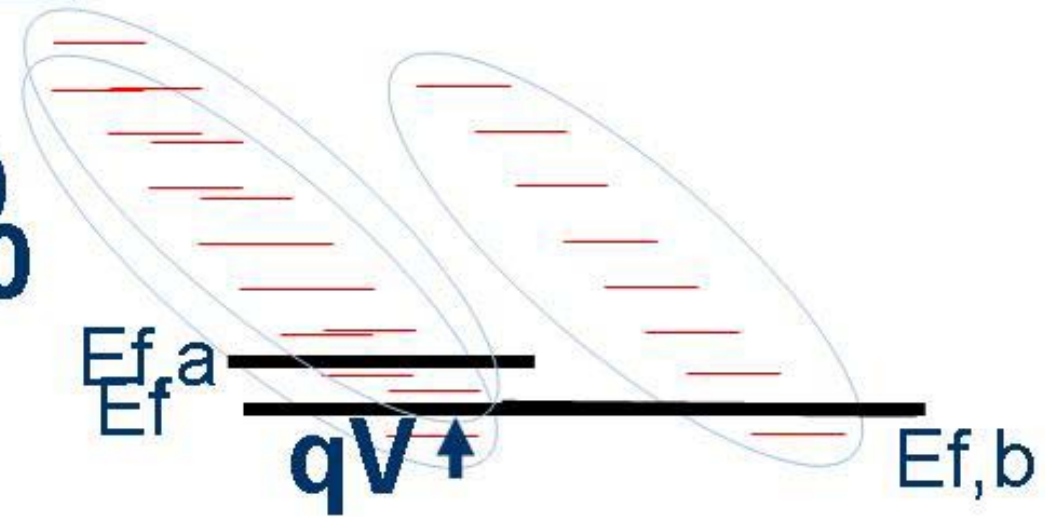


$$G_{ij} [\text{inter}] \sim 10^{18} \text{ m}^{-2}\text{s}^{-1}$$

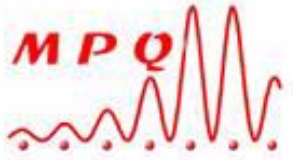


$$V \geq 0$$

$$= 0$$



ITQW 2007





⇒ 3 - The bias considered as a perturbation

$$G_{ij}^a(V) = \int_{\epsilon_j - \hbar\omega_{LO}}^{\infty} S_{ij}^a(E) f_A(E) (1 - f_B(E + \hbar\omega_{LO})) n_{opt} D(E) dE$$

The matrix elements do not depend on the very small applied bias

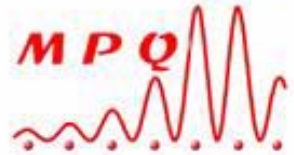
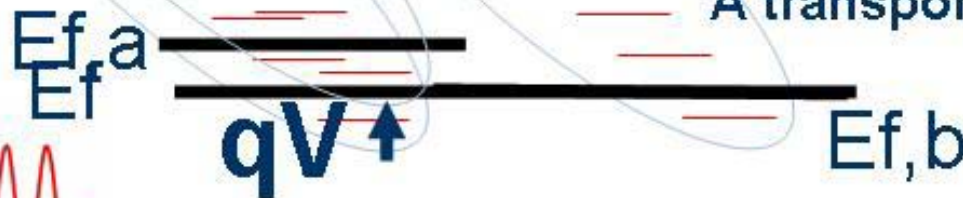
The bias breaks the Fermi level between subband i (cascade A) and subband j (cascade B)

These Fermi factors are different in G_{ij}^a and G_{ji}^e

$$G_{ij}^a \neq G_{ji}^e$$

A transport results from this non-equilibrium

$V > 0$
 $V = 0$



This document and any other information included herein are the property of Thales. They cannot be reproduced, transmitted, disseminated, stored in a retrieval system, or used in any way without the prior written permission of Thales. Model version: 10.2



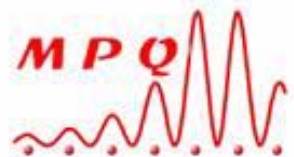
$$J = q \sum_{i \in A} \sum_{j \in B} (G_{ij}(V) - G_{ji}(V)) = q \sum_{i \in A} \sum_{j \in B} G_{ij}^{eq} \frac{qV}{k_B T}$$

$$\Rightarrow R_0 A = \frac{k_B T}{q^2 \sum_{i \in A} \sum_{j \in B} G_{ij}^{eq}}$$

Einstein Relation

$$\frac{D}{\mu} = \frac{k_b T}{q} \quad \text{with} \quad D = \frac{l^2 \sum_{i \in A} \sum_{j \in B} G_{ij}^{eq}}{n_{2D}}$$

* C. Koeniguer et al., Phys. Rev. B, 74, 235325 (2006)





The resistivity depends only on :

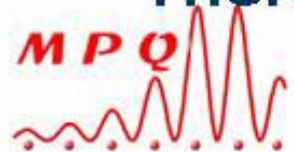
$$R_0 A = \frac{k_B T}{q^2 \sum_{i \in A} \sum_{j \in B} G_{ij}^{eq}}$$

- the doping concentration
- the physical parameters of the sample (thickness of the wells and barriers, materials constants like effective masses or Al percentage ...)

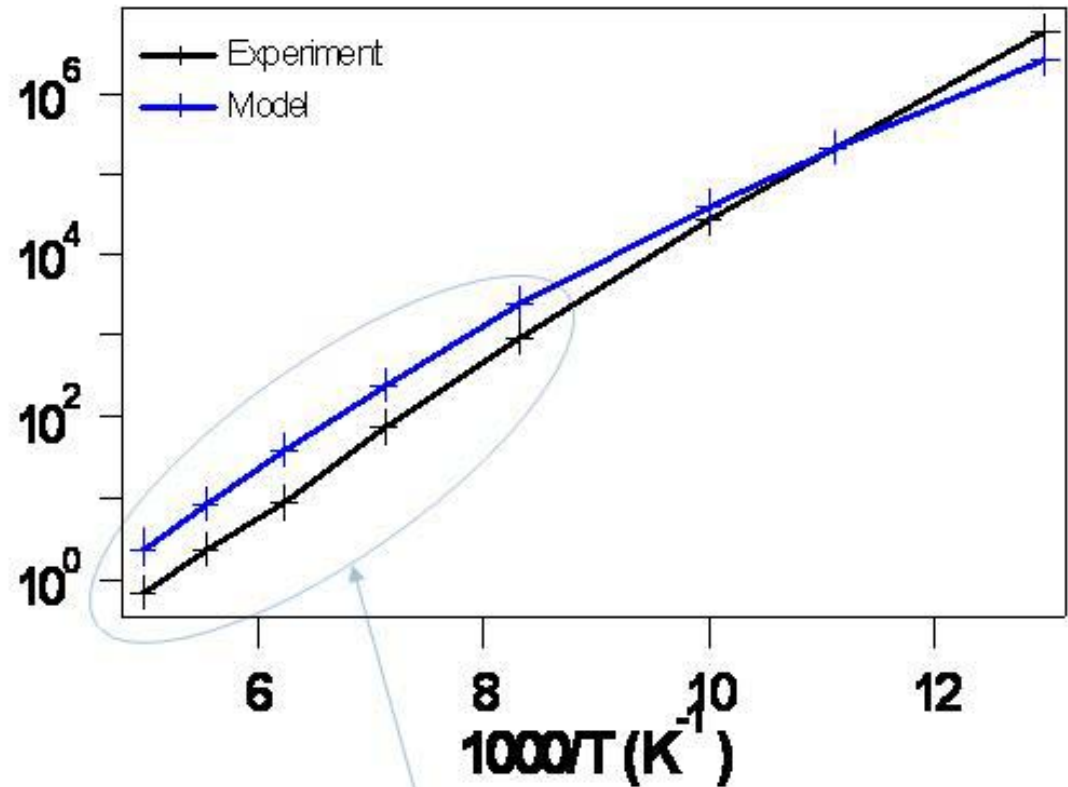
which are include in the G_{ij} terms :

$$G_{ij}^a(V) = \int_{\epsilon_j - \hbar\omega_{LO}}^{\infty} S_{ij}^a(E) f_A(E) (1 - f_B(E + \hbar\omega_{LO})) n_{opt} D(E) dE$$

There is no other adjustable parameters (no fit parameters)



$R_0 A$ ($\Omega \cdot \text{cm}^2$)



- less than one order of magnitude
- The differences are due to :
 - the differences between the expected and the real structure
 - the hypotheses of the model concerning the scattering mechanism

At high temperature, activation energy is in good agreement with the experiment

But there is no fit parameters





- True photovoltaic use
- Long integration times (no dark current)

The user

- Spectral band
- Working distance
- Integration time
- Pixel size
- Working temperature

Number of incident photons

Max. number of stockable electrons

Q

The structure

- Doping level
- Applied bias (in a QWIP)
- Working temperature

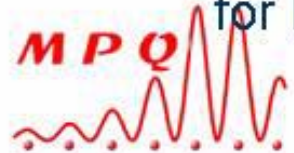
Photo electrons

Dark electrons

$< Q$

This condition usually limits the doping level and/or the working temperature
This has nothing to do with the detectivity

QCDs can work at higher doping levels than QWIPs : it may be interesting for low photon number application (4 μm , long distance...)



- Performances of a QCD at $5.7 \mu\text{m}$:
 - Responsivity at peak at 120 K : 15 mA/W
 - High Resistivity : $5 \cdot 10^6 \Omega \cdot \text{cm}^2 @ 77 \text{ K}$
- Model for electronic transport :
 - No other adjustable parameters except the doping concentration and the constants of the materials
 - Gives a good approximation of the resistivity
 - This gives to the possibility of a calculation of the performances of the detector and the system during its design (as a function of number of wells, doping...)

Thank you for your attention.

